Membrane Electroporation: A Molecular Dynamics Simulation

Mounir Tarek
Equipe de dynamique des assemblages membranaires, Unité Mixte de Recherche, Centre National de la Recherche Scientifique/ Université-Henri Poincaré 7565, Université Henri-Poincaré, 54506 Vandœuvre-lès-Nancy, France

ABSTRACT We present results of molecular dynamics simulations of lipid bilayers under a high transverse electrical field aimed at investigating their electroporation. Several systems are studied, namely 1), a bare bilayer, 2), a bilayer containing a peptide nanotube channel, and 3), a system with a peripheral DNA double strand. In all systems, the applied transmembrane electric fields (0.5 $V.nm^{-1}$ and 1.0 $V.nm^{-1}$) induce an electroporation of the lipid bilayer manifested by the formation of water wires and water channels across the membrane. The internal structures of the peptide nanotube assembly and that of the DNA strand are hardly modified under field. For system 2, no perturbation of the membrane is witnessed at the vicinity of the channel, which indicates that the interactions of the peptide with the nearby lipids stabilize the bilayer. For system 3, the DNA strand migrates to the interior of the membrane only after electroporation. Interestingly enough, switching of the external transmembrane potential in cases 1 and 2 for few nanoseconds is enough to allow for complete resealing and reconstitution of the bilayer. We provide evidence that the electric field induces a significant lateral stress on the bilayer, manifested by surface tensions of magnitudes in the order of 1 $mN.m^{-1}$. This study is believed to capture the essence of several dynamical phenomena observed experimentally and provides a framework for further developments and for new applications.

INTRODUCTION

The application of high electric fields to cells or tissues permeabilizes the cell membrane and is thought to produce aqueous-filled pores in the lipid bilayer (Crowley, 1973; Dimitrov, 1984; Glaser et al., 1988; Needham and Hochmuth, 1989; Teissié et al., 1999; Zimmerman, 1996; Zimmermann et al., 1976). This process, first observed for planar bilayer lipid membranes (Abidor et al., 1979; Benz et al., 1979), is referred to as membrane breakdown, electropermeabilization, or electroporation (Tsong, 1991; Weaver, 1995). It finds today numerous applications since, under certain conditions, it is reversible and hence permits efficient transmembrane transfer of small molecules (Teissié, 2002). Electroporation is routinely used in molecular biology and biotechnology and has recently found applications in medicine (Golzio et al., 2002; Harrison et al., 1998; Lee et al., 1992; Lundqvist et al., 1998; Mir et al., 1995; Neumann et al., 1982; Nishi et al., 1996). The method is also efficient for transdermal drug delivery and the transport of drugs, oligonucleotides, antibodies, and plasmids across cell membranes (Neumann et al., 1999; Prausnitz et al., 1993; Suzuki et al., 1998; Tsong, 1983, 1987).

Electroporation is witnessed when the lipid membrane is subject to transmembrane (TM) potentials of the order of a few hundred millivolts. The electroporation threshold depends on the composition of the bilayer. It can be modified by addition of amphiphilic surfactants. For instance, addition of polaxomer, a triblock anionic copolymer, increases the electroporation threshold and facilitates the membrane resealing, a property that is beneficial for minimizing electrical tissue injuries (Schmolka, 1994). In opposition, the presence of polyoxyethylene (CnEm) surfactants lowers the electroporation threshold. These may therefore be used as additives in biotechnological applications such as transdermal drug delivery to avoid thermal tissue injuries due to application of high electrical shocks (Lee and Kolodney, 1987). The intrinsic properties of the lipid membrane and its constituents may influence the electroporation threshold. Whereas cholesterol increases the electroporation threshold (Needham and Hochmuth, 1989), lysophosphatidylcholine has an opposite effect (Chernomordik et al., 1987). Membrane proteins may also influence the stability of the membrane under an external electric field. Because of their interactions with lipids, integral membranes are shown, for instance, to modulate the bilayer resealing as it has been demonstrated for gramicidin (Troiano et al., 1999).

To date, the molecular processes involved in membrane electroporation are still poorly known. The aim of our study is to bring about a detailed molecular level picture of the phenomena, using molecular dynamics (MD) simulations. In very recent investigations, several key aspects of the electropermeabilization process were revealed from multi-nanoseconds MD simulations of lipid bilayers. It was shown that under a high electric field, 0.5 $V.nm^{-1}$ and above, pore formation can be induced in bilayers on a nanosecond timescale (Tieleman et al., 2003). In a more detailed and recent study (Tieleman, 2004), it was found that for a large enough system, multiple pores with sizes up to 10 nm form independently. The simulations have evidenced that the electroporation process takes place in two stages. First, water molecules organized in single file like wires penetrate the hydrophobic core of the bilayer. This water penetration is

Submitted July 28, 2004, and accepted for publication March 8, 2005.

Address reprint requests to Mounir Tarek, E-mail: mtarek@edam.uhp-nancy.fr.

0006-3495/05/06/4045/09 $2.00

doi: 10.1529/biophysj.104.050617

apparently favored by local defects in the lipid headgroup region. Then, the water wires grow in length and expand into water-filled pores. These pores are stabilized by lipid headgroups that migrate from the membrane-water interface to the middle of the bilayer. It is suggested that water wires formation, the precursor to full electroporation, is driven by local field gradients at the water-lipid interface.

According to Tieleman's investigation, qualitatively, the pore formation does not seem to depend on the nature of the lipid headgroup. In fact, his MD simulations show that pores form even in the case of an octane layer sandwiched between water layers, i.e., in the absence of polar headgroups. This is consistent with experimental evidence on planar membranes of phosphatidylcholine and phosphatidylserine lipids (Diederich et al., 1998) that suggests that the rupture behavior, viz., membrane breakdown voltage and rupture kinetics are almost independent of the charges carried by the lipid headgroups. Similarly both previous simulations and experiments suggest that the electroporation process is independent of the ionic strength of the medium surrounding the membrane.

Here, after presenting rather similar results obtained independently by us, we address several key questions that remain open: 1), Do we observe resealing of the pores when the electric field is switched off? What is then the sequence of events? 2), What effect has the presence of a transmembrane channel on the process? and 3) What is the likely sequence of events that take place for translocation of a DNA plasmid placed near a membrane interface when the system is subject to the electric field?

To do so, we performed MD simulations of a bare bilayer, a bilayer containing a peptide nanotube channel, and a model membrane with a peripheral DNA double strand. In all cases, the applied voltage induced formation of water channels across the membrane that are stabilized by hydrophilic pores formed by participating lipid headgroups and acyl chains. The peptide channel is shown to stabilize the membrane due to its strong interaction with nearby lipids. The DNA strand migrates to the membrane interior only after electroporation of the bilayer. Interestingly, switching off the external transmembrane potential allows for complete resealing and reconstitution of the bilayer.

METHODS

Model systems

The membrane models used for this study are equilibrated fully hydrated dimyristoyl-phosphatidylcholine (DMPC) bilayers. At the temperatures set for the study, i.e., 300 K, the bilayer is in the biologically relevant liquid crystal L_α phase. We considered several systems. First, for the bare bilayer, we studied a small system consisting of 64 DMPC units and 1,645 water molecules. To investigate size effect, a larger system was constructed by replicating the system in the x and y directions of the water-bilayer interface, resulting in an assembly of 256 DMPC units.

The system containing the peptide channel was taken from Tarek et al. (2003). It consists of a nanotube formed of eight cyclo[(L-Trp-D-Leu)$_3$-L-Gln-D-Leu] subunits, organized in an antiparallel, β-sheetlike channel embedded in a hydrated DMPC bilayer (218 lipid molecules). Such cyclic peptides self-assemble into hollow tubular structures by means of a network of hydrogen bonds that connect the stacked subunits (Bong et al., 2001; Ghadiri et al., 1993). The complete system (synthetic channel, 215 lipid units, and 6,469 water molecules) represented a total of 46,097 atoms.

To investigate the effect of the external field on a short DNA strand located at the lipid-water interface, we considered a well-equilibrated palitoyl-oleyl-phosphatidylcholine (POPC) lipid bilayer (288 lipids), with excess water in which a 12 basepair 5′-cgcgaattcgcg-3′ ecor1 DNA duplex was placed in the aqueous phase near the lipid headgroups. The complete systems comprised the DNA duplex, 288 POPC lipids in united atoms representation, 14,500 water molecules, and 22 counterions to balance the DNA charges (total of 65,609 atoms). The number of lipid units and of water molecules considered is chosen such that the size of the system precludes interactions between the DNA strand and its images due to the use of periodic boundary conditions in the simulation. POPC was chosen for convenience as preequilibrated configurations of a united-atom model of a phosphatidylcholine lipid were at hand.

Simulation details

The MD simulations presented here were carried out using the program NAMD targeted for massively parallel architectures (Bhandarkar et al., 2002; Kale et al., 1999). All systems were examined in the (*NPT*) ensemble using three-dimensional periodic boundary conditions. The equations of motion were integrated using the multiple time-step algorithm (Izaguirre et al., 1999, 2001; Martyna et al., 1996). A Langevin piston was used to maintain the pressure at 1 atm. The temperature of the system was fixed at 300 K. Long-range, electrostatics forces were taken into account using the particle mesh Ewald approach (Darden et al., 1993; Essmann et al., 1995). The water molecules were described using the TIP3P model. Bond stretching, valence angle deformation, and torsional and nonbonded parameters of the cyclic peptides forming the nanotube, of the DNA nucleic acids, and of the DMPC and POPC lipid units were extracted from the all-atom CHARMM force field (MacKerell et al., 1998). The united atoms approximation was used for the POPC lipid acyl chains. The similarities of results presented in the following for simple lipid bilayers and those obtained by Tieleman (2004) indicate that the results are not highly dependant on the details of the simulation algorithms or of the force field used.

In experiments, a potential difference ΔV may be imposed by means of a voltage clamp or a pulse. In simulations, due to the small sizes of the systems and the use of periodic boundary conditions, it is impossible to impose a TM voltage by simple addition of explicit ions to the solution at both sides of the bilayer (Roux, 1997; Tieleman et al., 2001) Here, we adopted the same strategy as in Tieleman et al. (2001), i.e., applied an external electric field perpendicular to the membrane plane to maintain a fixed voltage difference across the bilayer (Tieleman et al., 2003, 2004). In practice, this is done by adding a force on all the atoms bearing a charge q_i, $F = q_i E$, where E is the constant external electric field.

For the analysis of the electrostatic properties of membrane, we recorded the electrostatic potential across the bilayer as the electroporation of the bilayer is taking place. This potential may be estimated using Poisson's equation and derived from the MD simulation as a double integral of $\rho(Z)$, the molecular charge density distributions at Z, following

$$\Delta\phi(Z) = \phi(Z) - \phi(0) = \frac{1}{\varepsilon_0}\int_0^Z\int_0^{Z'} \rho(Z'')dZ''\,dZ',$$

neglecting therefore the explicit electronic polarization (Tieleman et al., 1997; Tobias et al., 1997). Phosphadilylcholine headgroups have a large dipole moment. In hydrated bilayers, the orientation of the lipid headgroups with respect to the membrane surface is often found to average around 30°. This causes a nonnegligible local electric field that is partially compensated

by a specific orientation of interfacial water molecules and results in a net dipole potential across each interface (Cheng et al., 2003; Gawrisch et al., 1992; Shinoda et al., 1998), i.e., between the interior of the hydrocarbon layer and the aqueous phase. For this study, and in contrast to previous simulations (Berger et al., 1997; Tieleman et al., 1997; Tobias, 2001), we consider the dipole across the whole membrane. Owing to the symmetry of the bilayer and in the absence of salt, the total dipole across the bilayer is null. When an external electric field is applied, one expects that water molecules and lipid headgroups reorient, changing therefore the electrostatic properties of the membrane and hence the measured total dipole potential.

In agreement with Tieleman (2004), we find that the applied electric field E induces a voltage difference over the whole system $\Delta\phi(L_z) \approx |E|.L_z$ where L_z is the size of the simulation box in the direction perpendicular to the applied field. For instance, as we will see later, in the case of the bare lipid bilayers ($L_z \approx 64$ Å at rest) the total potential drop across the systems is ~3 and 6 V for the applied fields of intensity E = 0.5 V.nm^{-1} and 1.0 V.nm^{-1}, respectively.

Except for the system containing the peptide nanotube where the initial configuration was taken from our previous work, the two other systems were first equilibrated without application of the transverse electric field to afford initial configurations. The lengths of the various simulations ranged from 5 to 10 ns, depending on the system and the trajectories as will be indicated below for each system. As we will see in the following, these timescales are long enough for the electroporation to occur.

RESULTS

After the equilibration stage for all systems, external electric fields of magnitude $E = 0.5$ V.nm^{-1} and 1.0 V.nm^{-1} were applied in the direction perpendicular to the membrane. Fig. 1 depicts configurations taken from the simulations of model membranes subject to both TM voltages. In all cases, we observe the first of water fingers penetrating the hydrophobic core of the bilayer. As later confirmed by the analysis of the trajectories of all systems, and in agreement with Tieleman's observations (Tieleman, 2004), it appears that these fingers penetrate the bilayer hydrophobic core from either side of the bilayer, regardless of the direction of the applied field. These fingers expand toward the opposite interface or join other water fingers to ultimately form water wires that extend from one interface to the other of the bilayer hydrophobic core (Fig. 1 *b*). At a later stage, polar lipid headgroups migrate from the membrane-water interface to the interior of the bilayer, forming within hydrophilic pores that surround and stabilize the water columns as reported in the study by Tieleman (2004). These structures of the nonregular shapes of water channels are very different from the putative ''cylindrical lipid pores'' that are often postulated. This feature is also clear from previous MD simulations of membrane electroporation (Tieleman, 2004) and from MD simulations of permeation of membranes subject to mechanical stress (Leontiadou et al., 2004). Another noticeable fact brought by simulations is that despite the fact that the large water pores, after penetration of the lipid headgroup, are lined by ''hydrophilic polar heads'', a large fraction of the surface accessible to the solvent is in contact with lipid acyl chains (cf. Fig. 1 *e*).

Two bare fully hydrated bilayers containing, respectively, 64 and 256 lipid molecules were considered in this study.

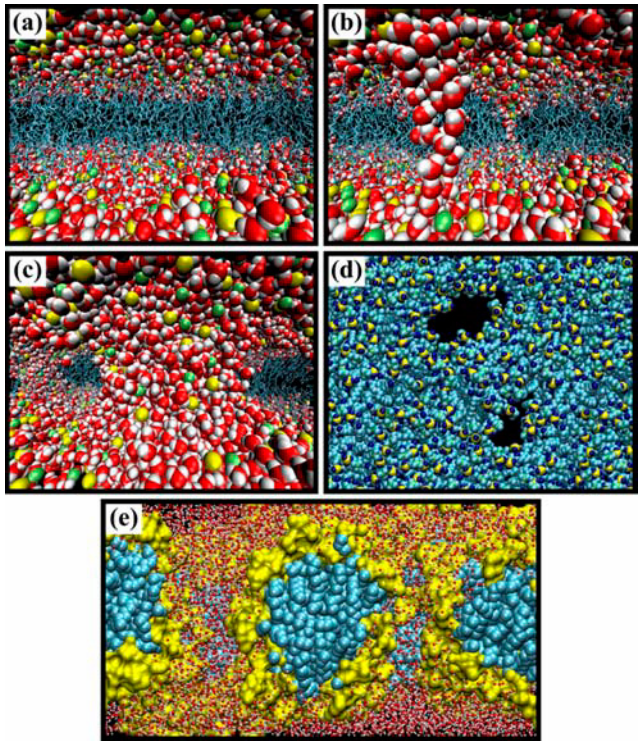

FIGURE 1 Configurations from the MD simulations for the large DMPC bilayer drawn in perspective. (*a*) Bilayer at equilibrium. (*b*) Formation of water wires at the initial stage of the electroporation process when the bilayer is subject to a transverse electric field. (*c*) Formation at a later stage of large water pores stabilized by lipid headgroups. Topology of the water pores (*d*) top view (*e*) side view. In the first three panels, water molecules (O, *red*; H, *white*), lipid phosphate (*yellow*), and nitrogen (*green*) atoms are represented by van der Walls radii, and the acyl chains (*cyan*) by stick representation. In the last panel, the hydrophilic lipid headgroup (*yellow*) and the hydrophobic acyl chains (*cyan*) are represented by van der Walls spheres to underline the topology and nature of the water pores. Due to the use of perspective views, atoms in the front appear bigger than those in the back.

Both systems underwent the same process, underlining the fact that that there is no size effect on the observed perturbations. The overall characteristics of the lipid bilayer—*A*, the average area occupied per DMPC molecule, and *d*, the system's repeat distance—appear not to be much perturbed as long as large water pores are not formed (cf. Fig. 2). As expected, a noticeable expansion of the membrane is observed subsequent to the large water pores formation. Note that *A* and *d* are somewhat coupled since water migrating from the bulk phase (decrease of *d*) penetrates the lipid core region (increase of *A*).

The kinetics of the membrane penetration of water fingers and of lipid headgroups is highly dependent, as expected, on the intensity of the applied field. Whereas at 0.5 V.nm^{-1} the first water fingers develop within a nanosecond (others in the case of large systems may appear later in the run), the same process is much faster (200 ps) for the 1.0 V.nm^{-1} run. Migration of the headgroups toward the interior of the bilayer takes longer (~4 ns and 1 ns, respectively for the

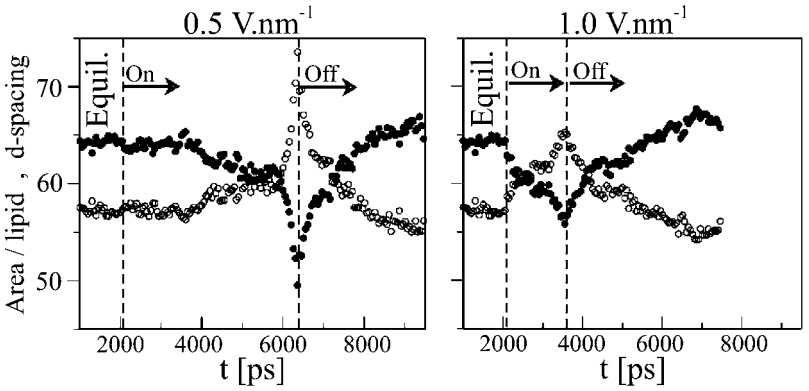

FIGURE 2 Evolution of A, the average area occupied per lipid (*open symbols*), and d, the bilayer d-spacing (*solid symbols*), for the DMPC bilayer system. Records along the simulations include the equilibration stage and the runs corresponding to the electroporation process and that corresponding to the resealing process, respectively, delimited by the vertical line indicating the onset of the field (*On*) and the offset (*Off*) or switching off of the field. The simulations corresponding to 0.5 and 1.0 V.nm^{-1} are displayed in the left and right panels, respectively.

bilayer subject to 0.5 V.nm^{-1} and 1 V.nm^{-1}). The latter may be traced back on Fig. 2, as the effect is a drastic expansion of the lipid patch.

After the fast reorientation of the water molecules dipole under action of the electric field, one notices a slower reorientation of the lipid headgroup dipoles. The reorientation of the phosphatidylcholine dipole during application of electric fields has been observed by electron spin resonance and NMR experiments (Stulen, 1981) and recently by infrared (Le Saux et al., 2001; Miller, 2002), which, in agreement with our data, shows that the conformation of the headgroups and more generally the properties of the interface are greatly affected by electroporation (Robello and Gliozzi, 1989).

To investigate the resealing process, the TM voltage was switched off after the membrane breakdown. Within a few nanoseconds, the lipid bilayers underwent a complete reconstitution. All water molecules forming the channel, as well as the lipid molecules in which headgroups were initially imbedded in the hydrophobic core, were expelled toward the lipid-water interface, and A and d nearly recovered their equilibrium resting state values (Fig. 2). Interestingly enough, the complete resealing of the bilayers for all systems studied occurs for all samples within 2–4 ns. This appears to be the upper limit for resealing of the largest pores formed in this study, i.e., those stabilized by the lipid headgroups, in absence of ions. One expects indeed that for a salt solution, these pores could be stabilized by the interactions between ions and the polar headgroups of the lipids. The lower bound for coalescence time in our study is recorded for the single-file water wires that span the membrane (hydrophobic pores). Those vanish by complete repartitioning at the interface within 250–500 ps depending on the shape of the wires.

The evolution of $\Delta\phi(Z)$, the intrinsic overall transmembrane electrostatic potential, as electroporation and resealing of the bilayer take place are reported in Fig. 3. Estimates from the MD trajectories show that the increase of $\Delta\phi(Z)$ to 3 and 6 V across the membrane is quasi-immediate after the application of the external field, as is the drop back to 0 V when the field is switched off. As indicated above, the voltage difference across the system is found, as in the investigation by Tieleman (2004), to satisfy $\Delta\phi(L_z) \approx |E| \times L_z$, where $L_z$is the size of the simulation box in the direction perpendicular to the applied field. The changes in the potential difference recorded for the system around the electroporation phenomena (large hole formation) is probably meaningless since such a quantity should depend on the concentration of holes in the system. It is noteworthy that

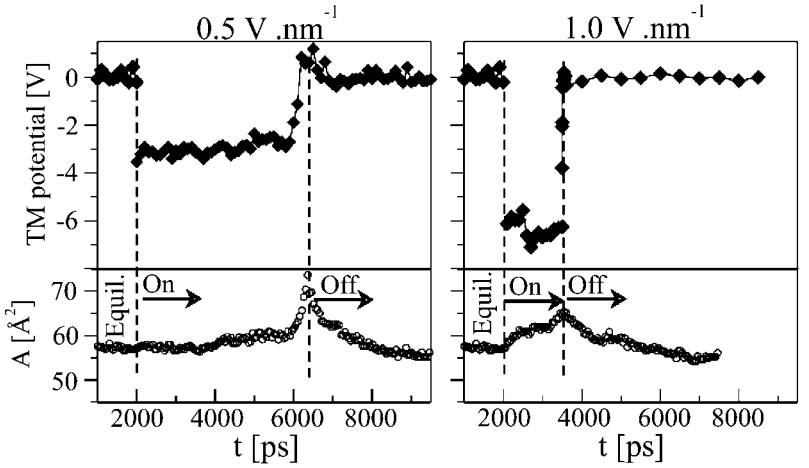

FIGURE 3 Evolution of A, the average area occupied per lipid (*open symbols*), and $\Delta\phi(Z)$, the intrinsic electrostatic potential across the membrane (*solid symbols*), during the electroporation process of the DMPC lipid bilayer. See Fig. 2 for caption details.

the changes in the potential due to the rearrangement of lipid headgroups, which is taking place at a much longer timescale, as well as the change due to the formation of water wires is very small compared to the large potential drop corresponding to polarization of the water, in agreement with Tieleman's observations (private communication).

Similar responses to the field were witnessed for the peptide nanotube/bilayer system (Fig. 4). However, no pore formation in the vicinity of the peptide channel was observed. The lipid molecules located nearby the peptide are known to strongly hydrogen bond to the peptide as previously reported (Tarek et al., 2003). Such interactions play a significant role in stabilizing those specific lipids. We can therefore speculate that at high membrane protein concentrations, the applied TM voltage necessary to break these hydrogen bonds should increase the electroporation threshold, which corroborates the experiments of Troiano et al. (1999) reporting on membrane/gramicidin stability.

The DNA/lipid system simulation was undertaken starting from a well-equilibrated 12-basepair 5′-cgcgaattcgcg-3′ ecor1 DNA duplex placed near a model POPC bilayer. We followed the perturbation of the system under a 1.0 V.nm^{-1} transverse electric field during 2 ns. During the MD trajectory, several pores formed in the bilayer, and the DNA duplex, the structure of which was hardly modified, diffused toward the interior of the membrane (Fig. 5). Once the DNA migrates to the bilayer core using the water pores beneath as a conduit, it comes in contact with lipid headgroups lining along the boundaries of the pore. At this stage, the interactions between the DNA and the membrane gave rise to a stable DNA/membrane complex as inferred from mediated gene delivery studies (Golzio et al., 2002).

We also considered a second starting configuration of the system where the DNA was displaced laterally. The results were quite different, as the electroporation of the membrane does not produce any water column just beneath the DNA. In this case translocation of the plasmid was not observed. The above results tend to indicate that local electroporation of the bilayer is a requisite to transmembrane transfer of species.

DISCUSSION

This study is aimed at investigating electroporation of lipid bilayer models using MD simulations. In agreement with experimental speculations, we witnessed formation of water wires and water channels in the hydrophobic domain of lipid bilayers when these are subject to an electrical field in the range 0.5–1.0 V.nm^{-1}. Permeation of the lipid core is initiated by formation of water wires that span the membrane. Those 'defects' grow in size, reaching the nanometer length scale, and drive the translocation of a few lipid headgroups toward the interior of the bilayer. The whole process takes place within a few nanoseconds and is more rapid for the highest field applied.

The configuration of the large pores indicates a rather nonuniform pathway with both hydrophilic and hydrophobic walls (cf. Fig. 1 *e*), formed by participating lipid headgroups and acyl chains. Such pores are large enough to serve as a conduit for ions and small molecules.

Under an electric field, reorientation of the solvent molecules at the bilayer-water interface is rather fast (a few picoseconds). This is followed by the slow reorientation of lipid headgroup dipoles, which appears to be the limiting step for complete reorganization of the bilayer, resulting in translocation of some lipid headgroups inside the hydrophobic membrane domain. Tieleman (2004) has recently observed a similar behavior. The simulations here presented show furthermore that switching off the applied field for a few nanoseconds is enough to allow complete resealing and reconstitution of the membrane bilayer. The limiting step in this reverse process is now the dissociation of lipid headgroup-headgroup located in the membrane core. At the final stage of the resealing process, all are expelled toward the interface. Interestingly enough, as expected, this reorganization is random, i.e., leads to repartition of the lipid molecules independent of their initial location. The resealing of the pores in this study was achieved within a few nanoseconds. It is however important to note that the studied system did not contain ions that, if present in the pores,

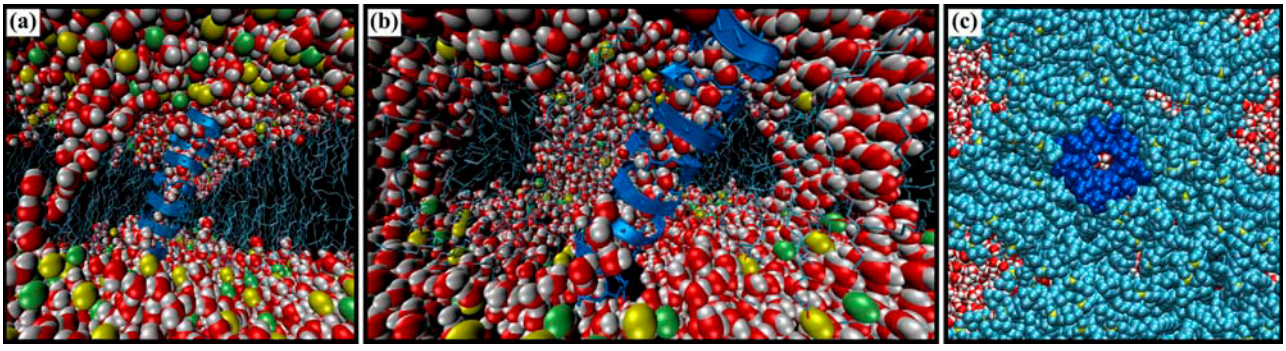

FIGURE 4 Configurations of the DMPC bilayer containing a peptide nanotube channel (*blue*) drawn in perspective from the MD simulation. (*a*) Initial, (*b*) side, and (*c*) top views of the system at the final stages of the electroporation process under a transverse field of magnitude 1.0 V.nm^{-1}. Note the absence of large water pores in the vicinity of the transmembrane channel.

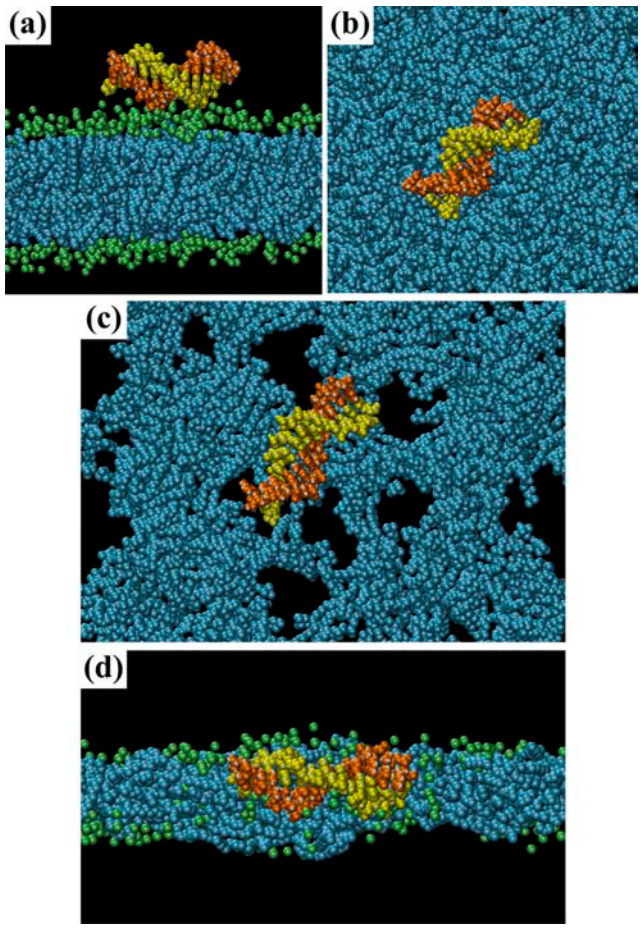

FIGURE 5 Configuration (*top* and *side views*) of the DNA/lipid system without external field (*a* and *b*) and after 2 ns of MD simulations (*c* and *d*) of application of the transverse electric field of magnitude 1.0 V.nm^{-1} drawn in perspective. Note that after electroporation of the membrane, the DNA duplex (*yellow* and *orange*) penetrates the lipid core using the existing pore beneath it and is stabilized by lipid headgroups (*green*).

would stabilize the latter for a much longer time. The very short time necessary for complete resealing of the model membrane seems, though, within orders of magnitude of estimates from experiments. These range from 100 ms (Melikov et al., 2001) to 100 s (Koronkiewicz et al., 2002). In both cases, the results of the data are interpreted in terms of a memory effect, in which, before resealing, the conductive pores, after turning off the electric pulse, transform to a nonconductive metastable state with long relaxation time. It is not clear whether the disagreement between our results and those inferred from experimental data is inherent to the samples used (salt solution, complex buffers, ...) or is due to size effects. Further simulations considering larger pores and salt are necessary to shed light on the kinetics of the resealing process.

To further quantify the effect of the electric field on the membranes, we analyzed their surface tension. It is well established that pore formation in membranes may also be induced by mechanical stress. Biomembranes have been shown to rupture at surface tensions in a range from ~1 to 25 mN.m^{-1} depending on the lipid composition (Bloom et al., 1991; Evans and Needham, 1987; Hallett et al., 1993; Mui et al., 1993; Needham et al., 1988; Olbrich et al., 2000). On the other hand, it has been recently argued (Lewis, 2003) that the electric field causes a lateral stress in the membrane that directly influences the interfacial tension and therefore has a dominant role in determining headgroup packing and pore formation. Here it is possible to make use of computer simulation to estimate the lateral pressure exerted on a membrane when subject to a transverse electric field. In the MD simulations presented so far, the calculations were carried out at constant temperature and constant total pressure. In such a case, the system is allowed to relax and to adjust its size from the initial configuration, which permits an estimate of A, the area per lipid and hydrocarbon thickness, without imposing an external stress or a given value for A. Doing so, however, we impose that the surface tension of the system, given by $\gamma = \int [P_\perp - P_\parallel]\, dz$, where $P_\perp$ and $P_\parallel$ are, respectively, the lateral pressure and the pressure normal to the water-lipid interface, is essentially null. To verify that application of an electric field induces a surface tension and to roughly estimate the latter, a different scheme for the simulation must be used. One possibility is to use the well-equilibrated systems as a starting point and perform MD simulations under an electric field at constant volume, i.e., without allowing relaxation of the lateral pressure. We accordingly performed such calculations on the DMPC bilayer subject to transmembrane voltages of 0.5 V.nm^{-1} and 1.0 V.nm^{-1} where a single large pore was created in the system. These calculations reveal that electroporation of the bilayer in both cases occurs within the same timescales as for previous calculations. At equilibration, the surface tension of the system γ after breakdown of the bilayer amounts to, respectively, 1 and 2 mN.m^{-1}.

At this stage, we did not investigate the effect of the asymmetry of the bilayer induced by the field. One expects indeed that the torques on the interfacial lipid dipoles are not the same on both sides of the bilayer due to their orientations with respect to the applied field. This should contribute to the change in surface tension, and further careful investigations of pressure profiles across the bilayer are underway to quantify such effects. Such profiles would be very helpful in determining the interplay between asymmetry of the effect on the headgroups and the probability of water penetration through either interface into the hydrophobic core. We also point out that the surface tension calculated as above in the small system is likely to vary with system size and hole size and should therefore be interpreted with caution.

It is interesting, however, to note that the herein calculated strength of the surface tension induced by the electroporation is within the range of values known to produce pore formation in membrane systems. More calculations are underway to refine the data and to investigate on one hand the

case of multiple pores formation, where the importance of coupling between pores formation is to be considered (Neu and Krassowska, 2003; Smith et al., 2004) and, on the other hand, how the results vary with the lipid characteristics such as headgroup charges and the nature of the lipid tails that govern, respectively, the hydrophilic and hydrophobic interactions within the membrane. It is clear, however, that our results support the model proposed by Lewis (2003) that stresses the role played by a rather significant lateral component to the stress vector generated by the transverse electric field. It may be at the origin of the differences in rupture kinetics recorded between membranes composed of lipids with difference tail compositions, such as those found between diphytanoyl-DPh and palmitoyl-oleoyl-PO membranes (Diederich et al., 1998).

One remaining crucial question is how the induced lateral stress relaxes in a macroscopic system when a voltage pulse is applied. Regardless of the topology of the bilayer, i.e., in planar lipid membranes or in a liposome, one expects that such relaxation will depend on 1), on the size of the defect created, i.e., the voltage applied; 2), the density of pores; and 3), the composition of the membrane. One may speculate that short bursts would create hydrophobic pores that may vanish and close rapidly as the stress relaxes and would correspond to the occurrence of the so-called prepore (Melikov et al., 2001) and that in the case of formation of rather hydrophilic pores stabilized by participating lipid headgroups, relaxation of the stress alone is unlikely to trigger coalescence of the pore.

We investigated the possible origins of stabilization of a membrane by integral proteins observed experimentally (Troiano et al., 1999) by studying a system consisting of an ion channel embedded in a lipid bilayer. In this case, we observed that no large pores are created in the immediate vicinity of the channel. We attributed this to the stabilizing effect of the anchoring of the lipid headgroups to the channel's side chains. Other calculations, performed on different samples, are necessary to confirm such a hypothesis.

For the DNA/lipid system, we considered a small fragment of a realistic DNA strand. In in vitro applications, the use of such plasmids concerns rather long molecules, for which our results may be viewed as investigating the behavior of one extremity. The overall process of DNA translocation thought to take place agrees with our finding, as it shows that the plasmid is stabilized in the membrane core after electroporation. DNA migration from one side of the cell to another is beyond this study, and no calculation was carried out to follow the resealing process. Electroporation-mediated DNA delivery concerns much larger plasmids than the 12 basepairs construct considered here. Transfer of such plasmids is certainly a complex process for which all aspects may not be addressed by our simulations. For instance, our data do not rule out the existence of multiple noncontinuous contacts, i.e., the occluding interaction of DNA with many small electropores (Smith et al., 2004). Similarly, the results here obtained may be envisioned as an initial step to a sliding process that is initiated from one end of the strand and that occurs at much longer timescales (De Gennes, 1999).

In comparing two systems, we have shown that, under a high electric field, the DNA strand considered diffused toward the interior of the bilayer when a pore was created beneath it, and within the same timescale, it remained at the interfacial region when no pore was present. Diffusion of the strand toward the interior of the membrane leads to a complex DNA/lipid in which the lipid headgroups encapsulate the strand. The partial charges carried by the zwitterionic phosphatidylcholine groups of the lipids are known to be efficient for neutralizing the charges carried by the DNA (Bandyopadhyay et al., 1999). Such interactions between the plasmid and the lipid contribute to the effective screening of DNA charges and therefore to the stabilization of the complex. The process herein described provides support to the gene delivery model by Teissié and collaborators (Golzio et al., 2002), in which it is proposed that only localized parts of the cell membrane brought to the permeabilized state is competent for transfer and that the proper transfer of DNA—that does not require that the electric pulse is maintained—is preceded by an ''anchoring step'' connecting the plasmid to the permeabilized membrane that takes place during the pulse.

It is important to note that most of the systems under study are mimics of real membranes but do not explicitly contain ion populations (except for the DNA systems, to ensure electrical neutrality). In cells, the presence of ions on both sides of the membrane may lead to a somewhat different process, as they participate in the collapse of the electrostatic potential. In such a case indeed, application of electrical fields of magnitudes similar to those applied here would lead to repartition of ions and charged species that ultimately contribute to the overall potential across the membrane. Furthermore, due to the use of periodic boundary conditions, the systems under study are, in fact, multilamellar stacks of lipid bilayers. To a certain extent, these results are more pertinent to the discussion of electroporation in the outermost Stratum Corneum skin tissues (Michaels et al., 1975).

The overall results here presented are believed to capture the essence of the several aspects of the electroporation phenomena in bilayers' membranes. It is noteworthy that electrical fields applied here, despite the fact that they are one magnitude higher than those applied experimentally for electroporation, do not lead to significant distortion of either the ion channel formed by hydrogen bonded stacks of peptide rings or the DNA fragment, which rationalizes the use of such techniques for a wide range of applications.

The author thanks the Centre National de la Recherche Scientifique for the poste rouge and the Action Thématique Anticipée sur Programme grant (2JE153). The Centre Informatique National de l'Enseignement Supérieur (CINES), Montpellier, France, is gratefully acknowledged for provision of generous amounts of CPU time on the SGI Origin 3800. Execution of NAMD2 was performed on 64 R14000 (500 MHz) processors of an SGI Origin 3800 at the CINES supercomputer center.

REFERENCES

Abidor, I. G., V. B. Arakelyan, L. V. Chernomordink, Y. A. Chimadzhev, V. F. Pastushenko, and M. R. Tarasevich. 1979. Electrical breakdown of BLM: main experimental facts and their qualitative discussion. *Bioelectrochem. Bioenerg.* 6:37–52.

Bandyopadhyay, S., M. Tarek, and M. L. Klein. 1999. Molecular dynamics study of lipid-DNA complexes. *J. Phys. Chem. B.* 103:10075–10080.

Benz, R., F. Beckers, and U. Zimmerman. 1979. Reversible electrical breakdown of lipid bilayer membranes—charge-pulse relaxation study. *J. Membr. Biol.* 48:181–204.

Berger, O., O. Edholm, and F. Jähnig. 1997. Molecular dynamics simulations of a fluid bilayer of dipalmitoylphosphatidylcholine at full hydration, constant pressure, and constant temperature. *Biophys. J.* 72: 2002–2013.

Bhandarkar, M., R. Brunner, C. Chipot, A. Dalke, S. Dixit, P. Grayson, J. Gullinsrud, A. Gursoy, W. Humphrey, D. Hurwitz, N. Krawetz, M. Nelson, and others. 2002. NAMD version 2.4. http://www.ks.uiuc.edu/Research/namd.

Bloom, M., E. Evans, and O. G. Mouristen. 1991. Physical properties of the fluid bilayer component of cell membranes. *Q. Rev. Biophys.* 24:293–397.

Bong, D. T., T. D. Clark, J. R. Granja, and M. R. Ghadiri. 2001. Self-assembling organic nanotubes. *Angew. Chem. Int.* 40:988–1011.

Cheng, J. X., S. Pautot, D. A. Weitz, and X. S. Xie. 2003. Ordering of water molecules between phospholipid bilayers visualized by coherent anti–Stokes Raman scattering microscopy. *Proc. Natl. Acad. Sci. USA.* 100: 9826–9830.

Chernomordik, L. V., S. I. Sukharev, S. V. Popov, V. F. Pastushenlo, A. V. Sokirov, I. G. Abidor, and Y. A. Chizmadzhev. 1987. The electrical breakdown of cell and lipid membranes: the similarity of phenomenologies. *Biochim. Biophys. Acta.* 902:360–373.

Crowley, J. M. 1973. Electrical breakdown of biomolecular lipid membranes as an electromechanical instability. *Biophys. J.* 13:711–724.

Darden, T., D. York, and L. Pedersen. 1993. Particle mesh Ewald—an Nlog(N) method for Ewald sums in large systems. *J. Chem. Phys.* 98: 10089–10092.

De Gennes, P.-G. 1999. Passive entry of a DNA molecule into a small pore. *Proc. Natl. Acad. Sci. USA.* 96:7262–7264.

Diederich, A., G. Bähr, and M. Winterhalter. 1998. Influence of surface charges on the rupture of black lipid films. *Phys. Rev. E.* 58:4883–4889.

Dimitrov, D. 1984. Electrical field-induced breakdown of lipid bilayers and cell membranes: a thin viscoelastic film model. *J. Membr. Biol.* 78: 53–60.

Essmann, U., L. Perera, M. L. Berkowitz, T. Darden, and L. G. Pedersen. 1995. A smooth particle mesh Ewald method. *J. Chem. Phys.* 103:8577–8593.

Evans, E., and D. Needham. 1987. Physical properties of surfactant bilayer membranes composed of lipids, cholesterol and polypeptides: thermal transitions, elasticity, cohesion and colloidal interactions. *J. Phys. Chem.* 91:4219–4228.

Gawrisch, K., D. Ruston, J. Zimmerberg, V. Parsegian, R. Rand, and N. Fuller. 1992. Membrane dipole potentials, hydration forces, and the ordering of water at membrane surfaces. *Biophys. J.* 61:1213–1223.

Ghadiri, M. R., J. R. Granja, R. A. Milligan, D. E. McRee, and N. Khazanovich. 1993. Self-assembling organic nanotubes based on a cyclic peptide architecture. *Nature.* 366:324–327.

Glaser, R. W., S. L. Leiken, L. V. Chernomordik, V. F. Pastushenko, and A. I. Sokirko. 1988. Reversible electrical breakdown of lipid bilayers: formation and evolution of pores. *Biochim. Biophys. Acta.* 940: 275–287.

Golzio, M., J. Teissie, and M.-P. Rols. 2002. Direct visualization at the single-cell level of electrically mediated gene delivery. *Proc. Natl. Acad. Sci. USA.* 99:1292–1297.

Hallett, F. R., J. Marsh, B. G. Nickle, and J. M. Wood. 1993. Mechanical properties of vesicles. II. A model for osmotic swelling and lysis. *Biophys. J.* 64:435–442.

Harrison, R. L., B. J. Byrne, and L. Tung. 1998. Electroporation-mediated gene transfer in cardiac tissue. *FEBS Lett.* 435:1–5.

Izaguirre, J. A., D. P. Catarello, J. M. Wozniak, and R. D. Skeel. 2001. Langevin stabilization of molecular dynamics. *J. Chem. Phys.* 114:2090–2098.

Izaguirre, J. A., S. Reich, and R. D. Skeel. 1999. Longer time steps for molecular dynamics. *J. Chem. Phys.* 110:9853–9864.

Kale, L., R. Skeel, M. Bhandarkar, R. Brunner, A. Gursoy, N. Krawetz, J. Phillips, A. Shinozaki, K. Varadarajan, and K. L. Schulten. 1999. NAMD2: Greater scalability for parallel molecular dynamics. *J. Comput. Phys.* 151:283–312.

Koronkiewicz, S., S. Kalinowski, and K. Bryl. 2002. Programmable chronopotentiometry as a tool for the study of electroporation and resealing of pores in bilayer lipid membranes. *Biochim. Biophys. Acta.* 1561:222–229.

Le Saux, A., J.-M. Ruysschaert, and E. Goormaghtigh. 2001. Membrane molecule reorientation in an electric field recorded by attenuated total reflection Fourier-transform infrared spectroscopy. *Biophys. J.* 80:324–330.

Lee, R. C., and M. S. Kolodney. 1987. Electrical injury mechanisms: dynamics of the thermal response. *Plast. Reconstr. Surg.* 80:663–671.

Lee, R. C., L. P. River, F. S. Pan, J. Li, and R. F. Wollman. 1992. Surfactant-induced sealing of electropermeabilized skeletal muscle membrane in vivo. *Proc. Natl. Acad. Sci. USA.* 89:4524–4528.

Leontiadou, H., A. E. Mark, and S. J. Marrink. 2004. Molecular dynamics simulations of hydrophilic pores in lipid bilayers. *Biophys. J.* 86:2156–2164.

Lewis, T. J. 2003. A model for bilayer membrane electroporation based on resultant electromechanical stress. *IEEE Trans. Dielec. Elec. Insul.* 10: 769–777.

Lundqvist, J. A., F. Sahlin, M. A. Aberg, A. Stromberg, P. S. Eriksson, and O. Orwar. 1998. Altering the biochemical state of individual cultured cells and organelles with ultramicroelectrodes. *Proc. Natl. Acad. Sci. USA.* 95:10356–10360.

MacKerell, A. D., Jr., D. Bashford, M. Bellott, R. L. Dunbrack Jr., J. Evanseck, M. J. Field, S. Fischer, J. Gao, H. Guo, S. Ha, D. Joseph-McCarthy, L. Kuchnir, and others. 1998. All-atom empirical potential for molecular modeling and dynamics studies of proteins. *J. Phys. Chem. B.* 102:3586–3616.

Martyna, G. J., M. E. Tuckerman, D. J. Tobias, and M. L. Klein. 1996. Explicit reversible integrators for extended systems dynamics. *Mol. Phys.* 87:1117–1157.

Melikov, K. C., V. A. Frolov, A. Shcherbakov, A. V. Samsonov, Y. A. Chizmadzhev, and L. V. Chernomordik. 2001. Voltage-induced non-conductive pre-pores and metastable single pores in unmodified planar lipid bilayer. *Biophys. J.* 80:1829–1836.

Michaels, A. S., S. K. Chandrasekaran, and J. E. Shaw. 1975. Drug permeation through human skin: theory and in vitro experimental measurements. *AIChE J.* 21:985–996.

Miller, I. R. 2002. Effect of electric field on the structure of phosphatidylcholine in a multibilayer system. *Bioelectrochemistry.* 57: 145–148.

Mir, L. M., S. Orlowski, J. Belehradek, J. Teissié, M. P. Rols, G. Sersa, D. Miklavcic, R. Gilbert, and R. Heller. 1995. Biomedical applications of electric pulses with special emphasis on transient antitumor electrochemotherapy. *Bioelectrochem. Bioenerg.* 38:203–208.

Mui, B. L.-S., P. R. Cullis, E. A. Evans, and T. D. Madden. 1993. Osmotic properties of large unilamellar vesicles prepared by extrusion. *Biophys. J.* 64:443–453.

Needham, D., and R. M. Hochmuth. 1989. Electro-mechanical permeabilization of lipid vesicles. *Biophys. J.* 55:1001–1009.

Needham, D., T. J. McIntosh, and E. Evans. 1988. Thermomechanical and transition properties of DMPC cholesterol bilayers. *Biochemistry.* 27: 4668–4673.

Neu, J. C., and W. Krassowska. 2003. Modeling postshock evolution of large pores. *Phys. Rev. E.* 67:021915.

Neumann, E., S. Kakorin, and K. Toensing. 1999. Fundamentals of electroporative delivery of drugs and genes. *Bioelectrochem. Bioenerg.* 48: 3–16.

Neumann, E., M. Schaefer-Ridder, Y. Wang, and P. H. Hofschneider. 1982. Gene transfer into mouse lyoma cells by electroporation in high electric fields. *EMBO J.* 1:841–845.

Nishi, T., K. Yoshizato, S. Yamashiro, H. Takeshima, K. Sato, K. Hamada, I. Kitamura, T. Yoshimura, H. Saya, J. Kuratsu, and Y. Ushio. 1996. High-efficiency in vivo gene transfer using intraarterial plasmid DNA injection following in vivo electroporation. *Cancer Res.* 56:1050–1055.

Olbrich, K., W. Rawicz, D. Needham, and E. Evans. 2000. Water permeability and mechanical strength of polyunsaturated phosphatidylcholine bilayers. *Biophys. J.* 79:321–327.

Prausnitz, M. R., V. G. Bose, R. Langer, and J. C. Weaver. 1993. Electroporation of mammalian skin: a mechanism to enhance transdermal drug delivery. *Proc. Natl. Acad. Sci. USA.* 90:10504–10508.

Robello, M., and A. Gliozzi. 1989. Conductance transition induced by an electric-field in lipid bilayers. *Biochim. Biophys. Acta.* 982:173–176.

Roux, B. 1997. Influence on the membrane potential on the free energy of an intrinsic protein. *Biophys. J.* 73:2980–2989.

Schmolka, I. R. 1994. Physical basis for polaxamer interactions. *Ann. N. Y. Acad. Sci.* 720:92–97.

Shinoda, W., M. Shimizu, and S. Okazaki. 1998. Molecular dynamics study on electrostatic properties of a lipid bilayer: Polarization, electrostatic potential, and the effects on structure and dynamics of water near the interface. *J. Phys. Chem. B.* 102:6647–6654.

Smith, K. C., J. C. Neu, and W. Krassowska. 2004. Model of creation and evolution of stable electropores for DNA delivery. *Biophys. J.* 86:2813–2826.

Stulen, G. 1981. Electric field effects on lipid membrane structure. *Biochim. Biophys. Acta.* 640:621–627.

Suzuki, T., B. C. Shin, K. Fujikura, T. Matsuzaki, and K. Takata. 1998. Direct gene transfer into rat liver cells by in vivo electroporation. *FEBS Lett.* 425:436–440.

Tarek, M., B. Maigret, and C. Chipot. 2003. Molecular dynamics investigation of an oriented cyclic peptide nanotube in DMPC bilayers. *Biophys. J.* 85:2287–2298.

Teissié, J. 2002. In vivo gene expression: combining hydrodynamic based transfection and electrotransfer. *Trends Biotechnol.* 20:487–488.

Teissié, J., N. Eynard, B. Gabriel, and M. P. Rols. 1999. Electropermeabilization of cell membranes. *Adv. Drug Deliv. Rev.* 35:3–19.

Tieleman, D. P. 2004. The molecular basis of electroporation. *BMC Biochem.* 5:10.

Tieleman, D. P., J. H. C. Berendsen, and M. S. P. Sansom. 2001. Voltage-dependent insertion of alamethicin at phospholipid/water and octane water interfaces. *Biophys. J.* 80:331–346.

Tieleman, D. P., H. Leontiadou, A. E. Mark, and S. J. Marrink. 2003. Molecular dynamics simulation of pore formation in phospholipid bilayers by mechanical force and electric fields. *J. Am. Chem. Soc.* 125: 6382–6383.

Tieleman, D. P., S. J. Marrink, and H. J. C. Berendsen. 1997. A computer perspective of membranes: molecular dynamics studies of lipid bilayer systems. *Biochim. Biophys. Acta.* 1331:235–270.

Tobias, D. J. 2001. Membrane simulations. *In* Computational Biochemistry and Biophysics. O. H. Becker, A. D. Mackerell Jr., B. Roux, and M. Watanabe, editors. Marcel Dekker, New York.

Tobias, D. J., K. Tu, and M. L. Klein. 1997. Atomic-scale molecular dynamics simulations of lipid membranes. *Curr. Opin. Colloid Int. Sci.* 2:15–26.

Troiano, G. C., K. J. Stebe, R. M. Raphael, and L. Tung. 1999. The effects of gramicidin on the electroporation of lipid bilayers. *Biophys. J.* 76: 3150–3157.

Tsong, T. Y. 1983. Voltage modulation of membrane permeability and energy utilization in cells. *Biosci. Rep.* 3:487–505.

Tsong, T. Y. 1987. Electric modification of membrane permeability for drug loading into living cells. *Methods Enzymol.* 149:248–259.

Tsong, T. Y. 1991. Electroporation of cell membranes. *Biophys. J.* 60:297–306.

Weaver, J. C. 1995. Electroporation theory. *In* Methods in Molecular Biology. Humana Press, Clifton, NJ. 3–29.

Zimmerman, U. 1996. The Effect of High Intensity Electric Field Pulses on Eukaryotic Cell Membranes: Fundamentals and Applications. CRC Press, Boca Raton, FL.

Zimmermann, U., G. Pilwat, F. Beckers, and F. Riemann. 1976. Effects of external electrical fields on cell membranes. *Bioelectrochem. Bioenerg.* 3:58–83.